Inclusive single particle density in configuration space from the QCD-cascade in DLA approximation⋆

B. Ziaja[1,2,a]

[1] Institute of Physics, Jagellonian University, Reymonta 4, 30-059 Cracow, Poland (e-mail: beataz@thp1.if.uj.edu.pl)
[2] H. Niewodniczanski Institute of Nuclear Physics, Radzikowskiego 152, 31-342 Cracow, Poland

Abstract. The structure of the QCD gluonic cascade in configuration space is investigated. The explicit form of the inclusive single particle density matrix and single particle density in configuration space transverse coordinates is derived in the double logarithmic approximation (DLA) of QCD. The possible simplification of the multiparton density matrix formalism for DLA approach is found and discussed.

1 Introduction

The interest of the configuration space structure of a hadronic source has appeared primarily in intensity interferometry [1]. The technique was developed originally to estimate the dimension of distant astronomical objects. Since that time it has seen widespread application in subatomic physics, in particular in analysis of elementary particle collisions [2]. The standard HBT procedure involves introducing an ansatz describing the geometry of the particle source, on the basis of a physical model. Then it investigates its multiparticle characteristcs in momentum space. Many models of hadron production based on some phenomenological or theoretical constraints [2] have been considered; however, the question as to what is the configuration space structure of the QCD cascade when derived explicitly from the fundamental theory has not been addressed so far.

Recently, several groups have analysed in great detail the multiparton distributions in the QCD gluonic cascades [3]. The results of their investigations show that perturbative QCD [4] provides a powerful framework not only for the description of hard quark and gluon jets but also of much softer multiparticle phenomena. Although not understood theoretically, the hypothesis of parton-hadron duality [5] provides an apparently successful link between theoretical parton distributions and observed particle spectra. This prescription was extensively tested in single particle spectra (and total multiplicities) and found to be in a good agreement with the available data (see e.g. [6]). Recently, there have appeared indications that it may also work for multiparticle correlations [7]. These unquestion-

able successes invite one to study further consequences of the theory for processes of particle production.

At this point we would like to notice that, if one wants to exploit fully the quantum-mechanical aspects of the QCD cascade, it is necessary to study at first the multiparton **density matrix**. The multiparticle distributions calculated so far give only diagonal terms of the density matrix and thus represent a rather restricted (although very important) part of the information available from the theory.

It is perhaps important to stress that in contrast to what is usually believed, the interest in studying the multiparticle density matrix is not purely academic. Multiparticle densities in configuration space cannot be observed directly. However, as suggested in [8], the density matrix allows one to obtain the multiparticle Wigner functions, as well, and this allows one to make predictions about the shape and range of the HBT interference with clear experimental consequences.

In my previous paper [9] I investigated the multiparticle density matrix (DM) of the gluonic cascade produced in e^+e^- collision in the framework of double logarithmic (DLA) approximation [4], [10] of QCD. I proposed a generating functional to obtain integral equations for the multiparticle density matrix in the quasi-diagonal limit, i.e. if the energies and emission angles of particles are close to each other.

Here I will be presenting the technique for extracting physical information from the density matrix approach, deriving the explicit form of inclusive single particle density matrix and single particle density in configuration space. For the sake of simplicity, I will be restricting myself to a discussion of particle density dependence on the transverse space coordinate x_T. In solving the problem, first I will discuss the derivation of the inclusive single particle density matrix $d_P^{in}(k', k)$. I will prove that the terms in $d_P^{in}(k', k)$ which do not vanish for $k = k'$ are

a A fellow of the Foundation for the Polish Science '97

leading in the double logaritmic perturbative expansion when $\alpha_S \to 0$, momentum of quark (antiquark) P generating the gluonic cascade is large:
$P \to \infty$, so that $\alpha_S \ln P \to 0$, and the double logarithmic contributions of the form $\alpha_S \ln^2 P = const$ dominate. Taking into account these leading terms will allow me to obtain the explicit analytic form of the density matrix, and consequently the explicit form of the single particle density in configuration space. Finally, I will be analysing the physical properties of inclusive single particle density, and I hope to find them in agreement with intuitive physical expectations.

2 Density matrix formalism

2.1 Definition of the density matrix

In this paper I will concentrate on the single particle density in configuration space. I will be discussing it in relation to the QCD-parton cascade within the framework of double logarithmic approximation (DLA), using the density matrix formalism presented in [9]. Hence in this section I will recall the definition of the density matrix for a particle production process, and show the relation between the density matrix and particle density in configuration space. Our assumption is that all the produced particles are real, i.e. they are on a mass shell. If the production of m particles can be realized in different ways represented by a sample of Feynman diagrams, then the exclusive m-particle density matrix equals the product of total production amplitude $S(k_1, .., k_m)$ and its complex conjugate $S^*(k'_1, .., k'_m)$ as:

$$d^{ex}(k'_1, .., k'_m; k_1, .., k_m) = S^*(k'_1, .., k'_m)S(k_1, .., k_m);$$
(1)

where the total amplitude $S(k_1, .., k_m)$ is the sum of all contributions $S_{(D)}$ from Feynman diagrams (D) including phase space factors:

$$S(k_1, .., k_m) = \sum_D S^{(D)}(k_1, .., k_m) \prod_{i=1}^{m} (2\omega_{k_i})^{-1/2}.$$
(2)

For inclusive analysis one constructs the m-particle density matrix as a series of integrated n-particle exclusive densities in the form:

$$d^{in}(\mathbf{k'_1}, .., \mathbf{k'_m}; \mathbf{k_1}, .., \mathbf{k_m})$$
$$= \sum_{n=m}^{\infty} \frac{1}{(n-m)!} \int [dk]_{m+1...n}$$
$$\times d^{ex}(\mathbf{k'_1}, .., \mathbf{k'_m}, \mathbf{k_{m+1}}, .., \mathbf{k_n}; \mathbf{k_1}, .., \mathbf{k_n});$$
(3)

where $[dk]_{i...j} \equiv d^3 k_i .. d^3 k_j$. This construction scheme implies, that the diagonal elements of the density matrix are equal to particle densities in momentum space. There is also an obvious relation between the density matrix and particle density in real space. Remembering, that the

space-time multiparticle amplitude is the on-mass-shell Fourier transform of the momentum amplitude, i.e.

$$S(x_1, .., x_m) = \int [dk]_{1...m} e^{i\omega_{k_1} t_1 - i\mathbf{k_1}\mathbf{x_1}}.$$
$$.e^{i\omega_{k_m} t_m - i\mathbf{k_m}\mathbf{x_m}} S(k_1, .., k_m); \qquad (4)$$

where ω_{k_i} denotes the energy of the ith produced particle, for the multiparticle density $\rho^{ex/in}(x_1, .., x_m)$ we get the relation:

$$\rho^{ex/in}(x_1, .., x_m)$$
$$= \frac{1}{(2\pi)^{3m}}$$
$$\times \int [dk]_{1...m}[dk']_{1...m} \, d^{ex/in}(k'_1, .., k'_m; k_1, .., k_m) \qquad (5)$$
$$\times e^{i(\omega_{k_1} - \omega_{k'_1})t_1 - i(\mathbf{k_1} - \mathbf{k'_1})\mathbf{x_1}} .. e^{i(\omega_{k_m} - \omega_{k'_m})t_m - i(\mathbf{k_m} - \mathbf{k'_m})\mathbf{x_m}};$$

where the factor $\frac{1}{(2\pi)^{3m}}$ was introduced to get the proper normalization:

$$\int [dx]_{1...m} \rho^{ex/in}(x_1, .., x_m)$$
$$= \int [dk]_{1...m} \rho^{ex/in}(k_1, .., k_m).$$
(6)

2.2 Parton cascade in the double logarithmic approximation

The double logarithmic approach in momentum space [4], [10] gives a good qualitative description of the structure of the gluonic cascade. It accounts only for the leading DL contributions to the multiparticle cross section. Although emitted soft gluons violate the energy and momentum conservation rules, however, at high energies the approximation reproduces quite well the selfsimilar structure of the gluon radiation. Let us consider in the framework of DLA the gluonic cascade generated in e^+e^- collision. Multiparticle exclusive amplitude $S^{(D)}_{e_1..e_m}(k_1, .., k_m)$, describing the production of m soft gluons:

$$S^{(D)}_{e_1..e_m}(k_1, .., k_m)$$
$$= (-1)^n \, e^{-\frac{w(P)}{2}} \prod_{i=1}^{m} M_{P_i}(k_i) \, e^{-\frac{w(k_i)}{2}}; \qquad (7)$$

is a product of the m emission factors:

$$M_{P_i}(k_i) = g_S \frac{(e_i \cdot P_i)}{(k_i \cdot P_i)} \Theta_{P_i}(k_i) \, G_{P_i}; \qquad (8)$$

where:
$g_S = \sqrt{4\pi\alpha_s}$,
n is the number of gluons emitted of quark (antiquark),
$k_i = (\omega_i, \mathbf{k_i})$ denotes the 4-momentum of the ith soft gluon,
$e_i \equiv e_i^{(j)}$, $j = 0, \ldots, 3$ describes its polarization,
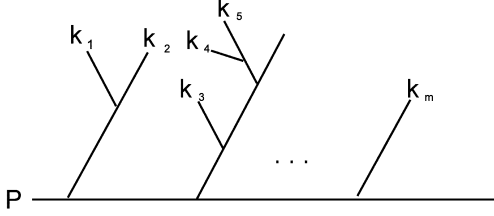P_i is the 4-momentum of the parent of the ith gluon,

Fig. 1. Feynman diagram for the production of m gluons in DLA, where P denotes the 4-momentum of the initial $q(\bar{q})$ and k_i denotes the 4-momentum of the ith produced gluon

G_{P_i} denotes the color factor for the given vertex of the tree diagram D, and can be conveniently represented as a tree diagram (see Fig. 1). Gluon emissions are not independent. Radiated particles have the memory of their parton parent, and of the previous parton splitting off its parent line. This dependence restricts the phase space of the produced gluon, and it is included in the form of a generalized step function $\Theta_{P_i}(k_i)$:

$$\Theta_P(k) := \{k^0 \equiv \omega < P^0,\ \theta_{\mathbf{kP}} < \theta,\ \omega\theta_{\mathbf{kP}} > Q_0\}; \quad (9)$$

where P is the momentum of the parent of a given parton k, θ denotes the emission angle of the previous parton splitting on the $P-$line, and Q_0 is a cut-off parameter. Virtual corrections appear as a radiation Sudakov factor $e^{-\frac{w(P)}{2}}$, where:

$$w(P) = \int d^3k\,\langle A_P^*(k)A_P(k)\rangle_{(e)} \quad (10)$$

denotes the total probability of emission of a gluon from the parent P, averaged over physical transverse polarizations e^1, e^2. $A_P(k)$ is given by:

$$A_P(k) = \frac{M_P(k)}{\sqrt{2\omega_k}}. \quad (11)$$

It should also be emphasized that produced gluons are real (on-mass-shell) particles, so the energy ω_k of a gluon of momentum k can be approximated as:

$$\omega_k = |\mathbf{k}| \equiv k. \quad (12)$$

Summing of the color factors G over the color indices gives the result:

$$G_{P_i}G_{P_i}^* = \begin{cases} C_F\ \text{dla}\ P_i = P \\ C_V\ \text{dla}\ P_i \neq P; \end{cases} \quad (13)$$

where P denotes the 4-momentum of the quark (antiquark) which initializes the gluonic cascade.

In DLA different tree diagrams come from different non-overlapping kinematic regions, and do not interfere. Therefore, to calculate exclusive and inclusive multigluon densities it is enough to sum up incoherently the squares of amplitudes (7). Hence one obtains the exclusive density $\rho_P^{ex}(\mathbf{k}_1,..,\mathbf{k}_m)$ in the form:

$$\rho_P^{ex}(\mathbf{k}_1,..,\mathbf{k}_m) \quad (14)$$
$$= e^{-w(P)} \sum_D \prod_{i=1}^m \langle A_{P_i}^*(k_i)A_{P_i}(k_i)\rangle_{(e_i)}\, e^{-w(k_i)};$$

Fig. 2. Generating functional (19) as a diagram series

parametrized by the momentum P of the quark (antiquark) which initializes the cascade. Multigluon inclusive density $\rho_P^{in}(\mathbf{k}_1,..,\mathbf{k}_m)$ follows from (3) as:

$$\rho_P^{in}(\mathbf{k}_1,..,\mathbf{k}_m) = \sum_{n=m}^{\infty} \frac{1}{(n-m)!} \quad (15)$$
$$\times \int [dk]_{m+1...n}\, \rho_P^{ex}(\mathbf{k}_1,..,\mathbf{k}_n).$$

Introducing the method of the generating functional (GF) (see [4] and references therein) allows us to perform the summation over diagrams in (14) and (15) in a very convenient way. While constructing the generating functional $Z_P[u]$, one applies explicitly the selfsimilarity property of the gluonic cascade. As a final result one obtains the recursive *master equation* in the form:

$$Z_P[u] = e^{-w(P)}\, exp\left(\int d^3k\,\langle A_P^*(k)A_P(k)\rangle_{(e)}\, u(k)Z_k[u]\right). \quad (16)$$

It can be proved [4] that equation (16) reproduces contributions of all tree diagrams D, and allows us to express multigluon densities $\rho_P^{in}(\mathbf{k}_1,..,\mathbf{k}_m)$ and $\rho_P^{ex}(\mathbf{k}_1,..,\mathbf{k}_m)$ as:

$$\rho_P^{ex}(\mathbf{k}_1,..,\mathbf{k}_m) = \frac{\delta^m}{\delta u_1 \ldots \delta u_m} Z_P\,|_{\{u=0\}}, \quad (17)$$

$$\rho_P^{in}(\mathbf{k}_1,..,\mathbf{k}_m) = \frac{\delta^m}{\delta u_1 \ldots \delta u_m} Z_P\,|_{\{u=1\}}; \quad (18)$$

where u_i denotes the probing function $u(k_i)$ and the functional derivative $\frac{\delta}{\delta u_i}$ denotes $\frac{\delta}{\delta u(k_i)}$ respectively.

We would like to emphasize the simplicity of the GF approach. Especially for inclusive densities the method allows us to skip the complicated summation procedure, and to express the required distribution in a simple, compact form (for details see [11]).

2.3 Density matrix in the DLA formalism

The DLA formalism in momentum space gives a good description of the structure of the gluonic cascade. The GF scheme allows to construct multigluon densities in a simple way. Since the method works so well for multiparticle distributions, one can expect to apply it successfully for other multiparticle observables. Below we briefly sum up the main results from [9] concerning calculation of the multiparticle density matrix in the framework of double logarithmic approximation.

First we derive the general expression for the exclusive and inclusive density matrices $d_P^{ex}(\mathbf{k}_1',..,\mathbf{k}_m';\mathbf{k}_1,..,\mathbf{k}_m)$
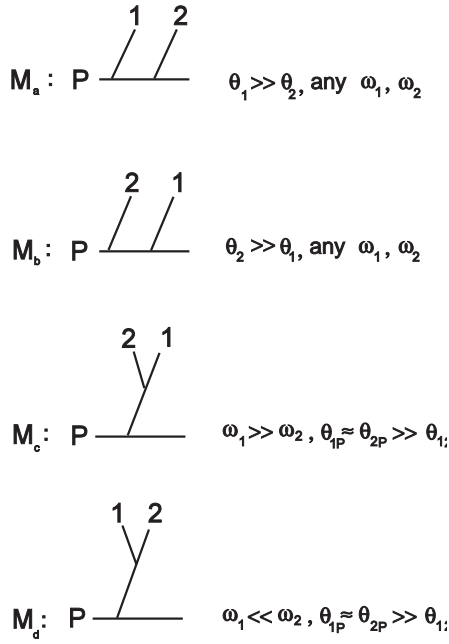
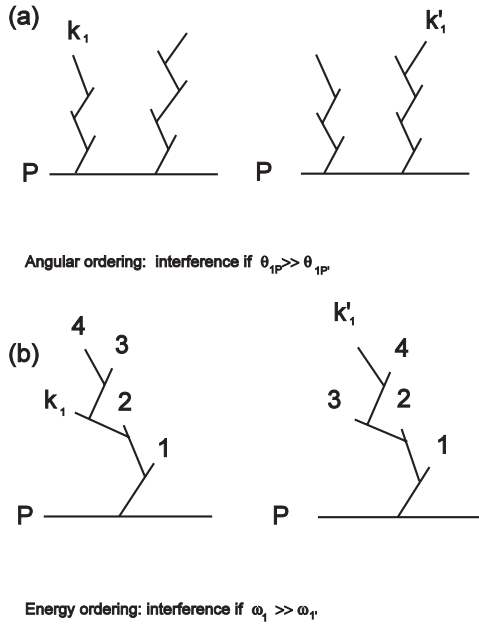**Fig. 3.** Redefined kinematical regions in DLA

Fig. 4. Interference between different diagrams for $d_P^{ex}(k_1', k_1)$. Remark: diagrams **a** and **b** are identical except of the position of k_1 (k_1') leg

and $d_P^{in}(\mathbf{k}_1', .., \mathbf{k}_m'; \mathbf{k}_1, .., \mathbf{k}_m)$. The task looks quite complicated because in this case the interference between different diagrams in (1), generally does not vanish. Let us define two functionals, $Z_P[u]$ and $Z_{P'}^*[w]$ (see Fig. 2), which generate the sum of all tree amplitudes and the sum of their complex conjugates respectively:

$$Z_P[u] = e^{-w(P)/2} exp(\int d^3k A_P(k)u(k)Z_k[u]),$$

$$Z_{P'}^*[s] = e^{-w(P')/2} exp(\int d^3k A_{P'}^*(k)s(k)Z_k^*[s]). \quad (19)$$

The multigluon density matrices can be then expressed as:

$$d_P^{ex}(\mathbf{k}_1', .., \mathbf{k}_m'; \mathbf{k}_1, .., \mathbf{k}_m)$$
$$= \frac{\delta^m}{\delta s_{1'} \dots \delta s_{m'}} \frac{\delta^m}{\delta u_1 \dots \delta u_m}$$
$$\times Z_P[u]Z_{P'}^*[s] \mid_{\{u=s=0\}, P=P'} , \quad (20)$$
$$d_P^{in}(\mathbf{k}_1', .., \mathbf{k}_m'; \mathbf{k}_1, .., \mathbf{k}_m)$$
$$= \frac{\delta^m}{\delta s_{1'} \dots \delta s_{m'}} \frac{\delta^m}{\delta u_1 \dots \delta u_m}$$
$$\times Z_P[u]Z_{P'}^*[s] \mid_{\{u=\frac{\delta}{\delta s}, s=0\}, P=P'} . \quad (21)$$

Equation (21) is, in fact, a complicated integral equation. The difficulty of the diagram summation does not disappear there. It is only hidden in the compact form of (21). However, we remember that in the above formula we have taken into account interference between *all* different graphs D and D'. And detailed analysis gives the result that in DLA not all the diagrams mix up: one can distinguish some interference classes. However, at the general level we did not succeed in formulation of such a GF which would take this fact into account.

Nevertheless, we do not need the most general form of the density matrix. We are interested in its behaviour when the differences of momenta $\mid k_1 - k_1' \mid, \ldots, \mid k_m - k_m' \mid$ are small, since we expect that large momentum differences will not contribute to Fourier transforms [12]. It can be shown that within this limit interferences between different diagrams vanish, and one sums up only "squared" contributions from identical graphs. In fact, from the analysis of the diagrams contributing to single particle density matrix $d_P^{ex}(k_1', k_1)$, it has been possible to prove (see Appendix A) that interference between different diagrams appears only if either energies or emission angles of produced particles are strongly ordered: $\omega_1 \gg \omega_{1'}$ ($\omega_1 \ll \omega_{1'}$) or $\theta_{1P} \gg \theta_{1'P}$ ($\theta_{1P} \gg \theta_{1'P}$). This statement can be generalized for any multiparticle density matrix (for proof see [9]).

Hence in our approximation we exclude mixing up different diagrams, and sum up only the squared contributions from identical ones. The exclusive and inclusive density matrices then take the simpler form:

$$d_P^{ex}(\mathbf{k}_1', .., \mathbf{k}_m'; \mathbf{k}_1, .., \mathbf{k}_m)$$
$$= \sum_D \prod_{i=1}^m (4\omega_{k_i'}\omega_{k_i})^{-1/2} \quad (22)$$
$$\times \langle S_{e_1..e_m}^{(D)}(k_1', \ldots, k_m')S_{e_1..e_m}^{(D)}(k_1, \ldots, k_m)\rangle_{(e_1..e_m)},$$
$$d_P^{in}(\mathbf{k}_1', .., \mathbf{k}_m'; \mathbf{k}_1, .., \mathbf{k}_m)$$
$$= \sum_{n=m}^\infty \frac{1}{(n-m)!} \sum_D \int [dk]_{m+1...n}$$
$$\times \prod_{i=1}^m (4\omega_{k_i'}\omega_{k_i})^{-1/2} \prod_{j=m+1}^n (4\omega_{k_j}\omega_{k_j})^{-1/2}$$
$$\times \langle S_{e_1..e_n}^{(D)}(k_1', \ldots, k_m', k_{m+1}, \ldots, k_n)$$

$$\times S^{(D)}_{e_1..e_n}(k_1,\ldots,k_n)\rangle_{(e_1..e_n)}. \tag{23}$$

The summation in (22), (23) over D can be easily performed using the generating functional which reproduces only contributions of identical tree diagrams. In [9] I proposed a master equation for such a generating functional (GF) $Z_{P'P}[u(k',k)]$. It accounts only for the contributions of "diagonal" diagrams, and generates the exclusive and inclusive density matrix as:

$$d^{ex}_P(\mathbf{k}'_1,..,\mathbf{k}'_m;\mathbf{k}_1,..,\mathbf{k}_m)$$
$$= \frac{\delta^m}{\delta u_{m',m}..\delta u_{1',1}} Z_{P'P}\mid_{\{u=0\},P=P'}, \tag{24}$$

$$d^{in}_P(\mathbf{k}'_1,..,\mathbf{k}'_m;\mathbf{k}_1,..,\mathbf{k}_m)$$
$$= \frac{\delta^m}{\delta u_{m',m}..\delta u_{1',1}} Z_{P'P}\mid_{\{u=\delta^3(l'-l)\},P=P'}. \tag{25}$$

The explicit form of its master equation, and the other formulae needed for further calculations are presented below. The GF reads:

$$Z_{P'P}[u] = e^{-W(P',P)} \sum_{n=0}^{\infty} \frac{1}{n!}$$
$$\times \int [dk']_{1...n}[dk]_{1...n}\, u(k'_1,k_1)..u(k'_n,k_n)$$
$$\times\langle A^*_{P'}(k'_1)A_P(k_1)\rangle_{(e_1)}..\langle A^*_{P'}(k'_n)A_P(k_n)\rangle_{(e_n)}$$
$$\times Z_{k'_1 k_1}[u]..Z_{k'_n k_n}[u]\, P_{1',..,n';1,..,n}; \tag{26}$$

where the function $P_{1',..,n';1,..,n}$ provides the requested parallel angular ordering (see Fig. 5) for n particles in the form:

$$P_{1',..,n';1,..,n} = \sum_{(i_1,..,i_n)\in Perm(1,..,n)}$$
$$\times\Theta(\theta_{k'_{i_1}P'} > .. > \theta_{k'_{i_n}P'})$$
$$\times\Theta(\theta_{k_{i_1}P} > .. > \theta_{k_{i_n}P}); \tag{27}$$

the product of the single particle amplitudes $\langle A^*_{P'}(k')A_P(k)\rangle_{(e)}$ averaged over gluon polarizations reads:

$$\langle A^*_{P'}(k')A_P(k)\rangle_{(e)}$$
$$\equiv A_{P'P}(k',k)$$
$$= \frac{4g^2_S}{2\pi} G^*_{P'}G_P \frac{1}{\sqrt{4\omega'^3\omega^3}} \frac{1}{\theta_{Pk}\theta_{P'k'}}\Theta_{P'}(k')\Theta_P(k); \tag{28}$$

and the radiation factor is given by:

$$W(P',P) = \frac{w(P') + w(P)}{2}. \tag{29}$$

The other notations are the same as in Sect. 2.2.

Generating functional (26) describes the sequence of "emissions": $\langle A^*_{P'}(k')A_P(k)\rangle_{(e)}$ of two particles k, k' from two parents P, P'. If the profile function $u(l',l)$ is equal to 0 and $\delta^3(l'-l)$ respectively, then the functional $Z_{P'P}$ takes the form:

$$Z_{P'P}[u=0] = e^{-W(P',P)},$$
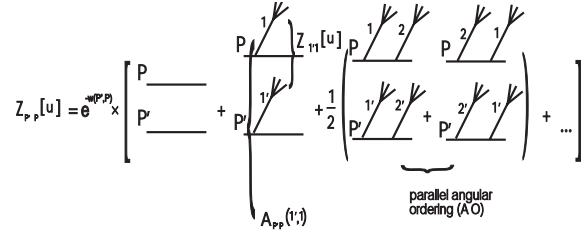$$Z_{PP}[u=\delta^3(l'-l)] = \quad 1. \tag{30}$$

Fig. 5. Master equation for generating functional (26) represented as a diagram series (for details see [9]). Function $P_{1',...,n';1,...,n}$ introduces the parallel angular ordering (AO)

For the profile function of the form $u(l',l) = v(l)\,\delta^3(l'-l)$ and $P = P'$ our $Z_{P'P}[u]$ reduces to functional (16), as expected:

$$Z_{PP}[u(l',l) = v(l)\,\delta^3(l'-l)] = Z_P[v(l)]. \tag{31}$$

2.4 Single particle density matrix. Leading terms

From relations (25), (26) one obtains a simple integral equation for the inclusive single particle density matrix:

$$d^{in}_P(k';k) = \int d^3s A_{PP}(s,s)d^{in}_s(k';k) \tag{32}$$
$$+f_P(k',k)A_{PP}(k',k)\, Z_{k',k}[u=\delta^3(l'-l)];$$

where $f_P(k',k)$ equals

$$f_P(k',k) = e^{-g^2_S C_F |\ln^2 \frac{\theta_{kPP}}{Q_0} - \ln^2 \frac{\theta_{k'PP}}{Q_0}|}. \tag{33}$$

Introducing the notation:

$$g_P(k',k) \equiv f_P(k',k)\, A_{PP}(k',k)$$
$$\times Z_{k',k}[u=\delta^3(l'-l)]; \tag{34}$$

we may write the symbolical solution $d^{in}_P(k',k)$ of (32) in the form:

$$d^{in}_P(k',k) = \sum_{n=0}^{\infty}\int d^3s_1\ldots d^3s_n\, A_{PP}(s_1,s_1)\ldots$$
$$\ldots A_{s_{n-1}s_{n-1}}(s_n,s_n)\, g_{s_n}(k',k). \tag{35}$$

We present (32), (35) as a final result obtained in [9]. The exact solution of $d^{in}_P(k',k)$ and its detailed properties will be discussed below. We may replace $A_{PP}(s,s)$ in (35) with its explicit form taken from (28):

$$d^{in}_P(k',k) = \sum_{n=0}^{\infty}(2b)^n \int \frac{ds_1}{s_1}$$
$$\times\int \frac{d\Omega_{s_1}}{2\pi\theta^2_{P1}}\Theta_P(s_1)\int \frac{ds_n}{s_n} \tag{36}$$
$$\times\int \frac{d\Omega_{s_n}}{2\pi\theta^2_{n-1,n}}\Theta_{s_{n-1}}(s_n)\, g_{s_n}(k',k);$$

where $\int d\Omega_{s_i}$ denotes the angular integration over the direction of vector $\mathbf{s_i}$, $\theta_{i,j} \equiv \theta_{s_i,s_j}$ and $b \equiv g_S^2 C_F$. Factor $g_s(k', k)$ defined by expression (34), reads:

$$
\begin{aligned}
&g_S(k', k) \\
&= \frac{2b}{2\pi} \frac{1}{\sqrt{k^3 k'^3}} \frac{1}{\theta_{Sk}\theta_{Sk'}} \Theta_S(k')\Theta_S(k) \\
&\times e^{-b|\ln^2 \frac{\theta_{kS}S}{Q_0} - \ln^2 \frac{\theta_{k'S}S}{Q_0}|} e^{-b'/2(\ln^2 \frac{k\theta_{kS}}{Q_0} + \ln^2 \frac{k'\theta_{k'S}}{Q_0})} \\
&\times \sum_{n=0}^{\infty} (2b')^n \int [dk]_{1...n} \frac{1}{2\pi\theta_{k1}\theta_{k'1}} \cdot \cdot \frac{1}{2\pi\theta_{kn}\theta_{k'n}} \frac{1}{k_1^3} \cdot \cdot \frac{1}{k_n^3} \\
&\times \Theta(\theta_{k1} > .. > \theta_{kn})\Theta(\theta_{k'1} > .. > \theta_{k'n}) \\
&\times \Theta_{k'}(1)..\Theta_{k'}(n)\Theta_k(1)..\Theta_k(n);
\end{aligned}
\tag{37}
$$

where $b' \equiv g_S^2 C_V$. The term which dominates in (37) in the double logarithmic approximation: $b \to 0$ ($b \propto \alpha_S$), $P \to \infty$, $b\ln \frac{P}{Q_0} \to 0$, and $b\ln^2 \frac{P}{Q_0} = const$, has the explicit form (for details see Appendix B):

$$
g_S^{(1)}(k', k) = \frac{2b}{2\pi} \frac{1}{\sqrt{k^3 k'^3}} \frac{1}{\theta_{Sk'}\theta_{Sk}} \Theta_S(k') \Theta_S(k).
\tag{38}
$$

Consequently, one may check (see Appendix B) that this term iterated in (37) produces the DLA leading contribution to the density matrix $d_P^{in}(k', k)$. Hence we may write finally that:

$$
\begin{aligned}
d_P^{in}(k', k) &\overset{DLA}{=} \sum_{n=0}^{\infty} (2b)^n \int \frac{ds_1}{s_1} \int \frac{d\Omega_{s_1}}{2\pi\theta_{P1}^2} \Theta_P(s_1) \\
&\cdots \int \frac{ds_n}{s_n} \int \frac{d\Omega_{s_n}}{2\pi\theta_{n-1,n}^2} \Theta_{s_{n-1}}(s_n) \\
&g_{s_n}^{(1)}(k', k).
\end{aligned}
\tag{39}
$$

The above result simplifies significantly the single particle density matrix approach [9]. We apply it in Sect. 4.2. so as to improve calculation of the single particle density in mixed coordinates.

3 DLA in configuration space

3.1 Fourier transform in transverse coordinates

The DLA soft parton cascade starts from the initial parton of momentum $\mathbf{P}$. Momenta of all particles produced from parton P refer to the $\mathbf{P}$ direction: they depend on the transverse and longitudinal momenta $\mathbf{k_T}$ and k_L (see e.g. [4], [13]) taken with respect to the $\mathbf{P}$ axis.

This dependence influences the structure of the cascade in configuration space. The single particle amplitude $S_P(x)$ (4) takes the form:

$$
\begin{aligned}
S_P(x) &= \int d^3k \, e^{i\omega t - i\mathbf{k}\mathbf{x}} S_P(\mathbf{k}) \\
&= \int dk_L d^2 k_T \, e^{i\omega t - i\mathbf{k}\mathbf{x}} S_P(\mathbf{k});
\end{aligned}
\tag{40}
$$

where $S_P(\mathbf{k})$ ($S_P(x)$) denotes the amplitude to produce a single particle with the momentum $\mathbf{k}$ (at the space-time coordinate x) from the initial particle of momentum $\mathbf{P}$, and the 3-dimensional product $\mathbf{k}\mathbf{x}$ reads:

$$
\mathbf{k}\mathbf{x} = k_L x_L + \mathbf{k_T}\mathbf{x_T};
\tag{41}
$$

where indices L and T denote longitudinal and transverse components of momenta and coordinates with respect to the $\mathbf{P}$ axis.

Using the approximation of small emission angles $\theta \ll 1$, consequently neglecting terms of order $P\theta^2$ and restricting to finite, small time intervals $t \ll (P\theta^2)^{-1}$ one may write approximate relations:

$$
k_L \approx \omega = |\mathbf{k}| \equiv k
\tag{42}
$$
$$
k_T \approx k\theta_{Pk}
\tag{43}
$$

Hence (40) can be rewritten as the product of 2 separate Fourier transforms: 1-dimensional FT of $(k_L, t - x_L)$, and 2-dimensional FT of $(\mathbf{k_T}, -\mathbf{x_T})$ in the form:

$$
\begin{aligned}
S_P(x_L, \mathbf{x_T}, t) &= \int dk \, e^{ik(t - x_L)} \\
&\times \int d^2 k_T \, e^{-i\mathbf{k_T}\mathbf{x_T}} S_P(k, \mathbf{k_T}).
\end{aligned}
\tag{44}
$$

Equation (44) gives us a good tool to investigate the space-time structure of DLA. We may now concentrate on particle distribution in transverse coordinates, which is physically the most interesting case. For the sake of simplicity, let us consider for $t = 0$ the single particle amplitude $S_P(k, \mathbf{x_T})$ in mixed transverse space and longitudinal momentum coordinates [13] defined as:

$$
S_P(k, \mathbf{x_T}, 0) = \int d^2 k_T \, e^{-i\mathbf{k_T}\mathbf{x_T}} S_P(k, \mathbf{k_T}).
\tag{45}
$$

For the single particle exclusive distribution $\rho_P^{ex}(k, \mathbf{x_T}, 0)$, defined as the amplitude square:

$$
\rho_P^{ex}(k, \mathbf{x_T}, 0) = |S_P(k, \mathbf{x_T}, 0)|^2;
\tag{46}
$$

one obtains simple expression in the form:

$$
\begin{aligned}
\rho_P^{ex}(k, \mathbf{x_T}, 0) &= \frac{1}{(2\pi)^2} \int d^2 k_T d^2 k'_T \\
&\times e^{-i(\mathbf{k_T} - \mathbf{k'_T})\mathbf{x_T}} d_P^{ex}(k, \mathbf{k'_T}; k, \mathbf{k_T}).
\end{aligned}
\tag{47}
$$

Relation (47) holds also for inclusive single particle density:

$$
\begin{aligned}
\rho_P^{in}(k, \mathbf{x_T}, 0) &= \frac{1}{(2\pi)^2} \int d^2 k_T d^2 k'_T \\
&\times e^{-i(\mathbf{k_T} - \mathbf{k'_T})\mathbf{x_T}} d_P^{in}(k, \mathbf{k'_T}; k, \mathbf{k_T});
\end{aligned}
\tag{48}
$$

and can be easily generalized for the multiparticle case. In this paper we study the inclusive single particle density in mixed coordinates $\rho_P^{in}(k, \mathbf{x_T}, 0)$ for the QCD gluonic cascade in DLA approximation.
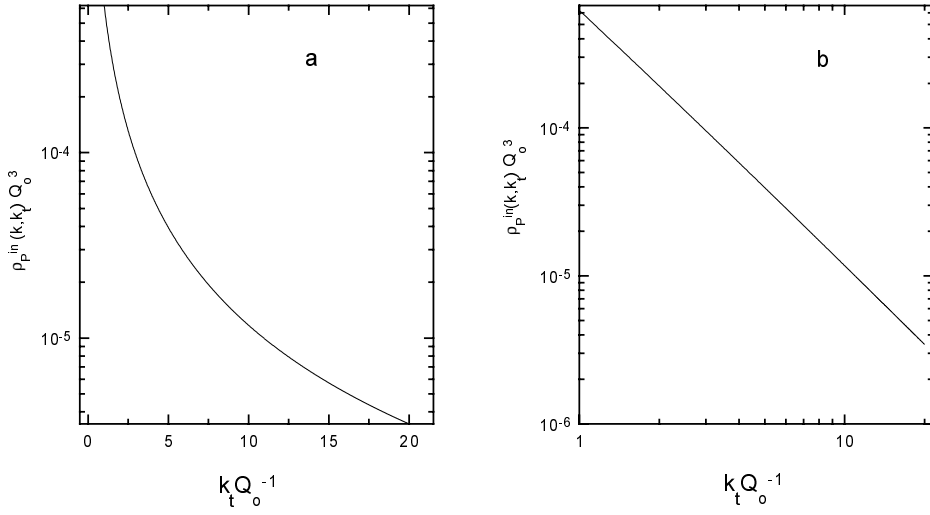
Fig. 6. Function $\rho_P^{in}(\mathbf{k})$ from (49) vs $k_T \equiv |\; \mathbf{k}_T\;|$ in Q_0 units for parameters $b = 0.25$, $P/Q_0 = 243$, $\theta = 1$, $k/Q_0 = 128$, chosen following [11]. The power fit reads $\rho_P^{in}(\mathbf{k}) = (\frac{k_T}{Q_0})^{-1.74} * 0.00065\, Q_0^{-3}$. Plot **a** with the logarithmic scale for the vertical axis, plot **b** with the logarithmic scale for both vertical and horizontal axes

4 Inclusive single particle density in configuration space

4.1 Physics

Momentum and configuration space description of a particle source are related to each other by the Fourier transform. Therefore one expects to extract from the observables in momentum space some qualitative information about their behaviour in configuration space. This observation applies, of course, to single particle density. In the DLA approach the inclusive single particle density $\rho_P^{in}(\mathbf{k})$ [11] reads:

$$\rho_P^{in}(\mathbf{k})$$
$$= \frac{2b}{2\pi} \frac{1}{k k_T^2} \sum_{n=0}^{\infty} \frac{(2b)^n}{(n!)^2} ln^n(\frac{P}{k}) ln^n(\frac{k_T}{Q_0})\, \Theta_P(k)$$
$$= \frac{2b}{2\pi} \frac{1}{k k_T^2} I_0\left(\sqrt{8b\, ln(\frac{P}{k}) ln(\frac{k_T}{Q_0})}\right)\Theta_P(k); \quad (49)$$

where $b \equiv g_S^2 C_F$. For constant k the $\rho_P^{in}(\mathbf{k})$ is concentrated around $\mathbf{P}$ direction (see Fig. 6) (skipping for now the $\Theta_P(k)$ limitations). We expect, that the single particle distribution $\rho_P^{in}(k, \mathbf{x}_T, 0)$ (48) in configuration space will be concentrated around the P direction, as well. However, it has to obey the uncertainty principle. Since there are cut-offs of form (9) in density matrix, its Fourier transform will contain some oscillations, due to the restricted integration region. Moreover, relation (6) implies, that both densities $\rho_P^{in}(\mathbf{k})$ and $\rho_P^{in}(k, \mathbf{x}_T, 0)$ have the same normalization, if integrated over d^3k and $dk\, d^2x_T$ respectively.

Remembering the above remarks, we propose now a technique for deriving the explicit form of inclusive single particle density in configuration space.

4.2 Single particle density

We may calculate the single particle density $\rho_P^{in}(k, \mathbf{x}_T, 0)$ (48) as a Fourier transform of DLA density matrix (39).

Let us make the transverse Fourier transform of both sides of (39). We obtain:

$$\rho_P^{in}(k, \mathbf{x}_{\mathbf{T(P)}}, 0)$$
$$\overset{\text{DLA}}{=} \frac{1}{(2\pi)^2} \int d^2 k_{T(P)} d^2 k'_{T(P)} e^{-i(\mathbf{k}_{T(P)} - \mathbf{k}'_{T(P)})\mathbf{x}_{\mathbf{T(P)}}}$$
$$\times \sum_{n=0}^{\infty} (2b)^n \int \frac{ds_1}{s_1} \int \frac{d\Omega_{s_1}}{2\pi\theta_{P1}^2} \Theta_P(s_1)$$
$$\ldots \int \frac{ds_n}{s_n} \int \frac{d\Omega_{s_n}}{2\pi\theta_{n-1,n}^2} \Theta_{s_{n-1}}(s_n)$$
$$\times g_{s_n}^{(1)}(k, \mathbf{k}'_{\mathbf{T(S)}}; k, \mathbf{k}_{\mathbf{T(S)}}); \quad (50)$$

where indices T(P),T(S) correspond to the reference frame with the $z-$axis placed along the $P\,(S)$ direction. The term of the lowest order $(n = 0)$ in (50) which is leading in DLA approximation takes then the form:

$$\rho_P^{in\,(1)}(k, \mathbf{x}_{\mathbf{T(P)}}, 0)$$
$$= \frac{1}{(2\pi)^2} \int d^2 k_{T(P)} d^2 k'_{T(P)} e^{-i(\mathbf{k}_{\mathbf{T(P)}} - \mathbf{k}'_{\mathbf{T(P)}})\mathbf{x}_{\mathbf{T(P)}}}$$
$$\times g_P^{(1)}(k, \mathbf{k}'_{\mathbf{T(S)}}; k, \mathbf{k}_{\mathbf{T(S)}}) \quad (51)$$
$$= \frac{2b}{2\pi} k\, \Theta(\frac{Q_0}{\theta} < k < P)(\int_{\frac{Q_0}{k}}^{\theta} d\theta_{Pk} J_0(x_T k\theta_{Pk}))^2.$$

The numerical plot of (51) is presented in Fig. 7. There is a limiting maximum value for $x_T = 0$, as expected, and for large x_T the function has a power decrease with the best fit exponent $x_T^{-3.07}$. The result confirms our intuitive analysis from Sect. 4.1. The term $\rho_P^{in\,(1)}(k, \mathbf{x}_{\mathbf{T(P)}}, 0)$ is concentrated around the **P** direction, however stronger than $\rho_P^{in\,(1)}(k, \mathbf{k}_{\mathbf{T}})$ from (49).

Derivation of terms of an arbitrary order in expansion (39) is more complicated. To proceed, let us analyse the last part of (39). It reads:

$$\int \frac{ds_n}{s_n} \int \frac{d\Omega_n}{2\pi\theta_{n-1,n}^2}\, \Theta_{n-1}(s_n)\, g_n^{(1)}(k, \mathbf{k}'_{\mathbf{T(S)}}; k, \mathbf{k}_{\mathbf{T(S)}})$$
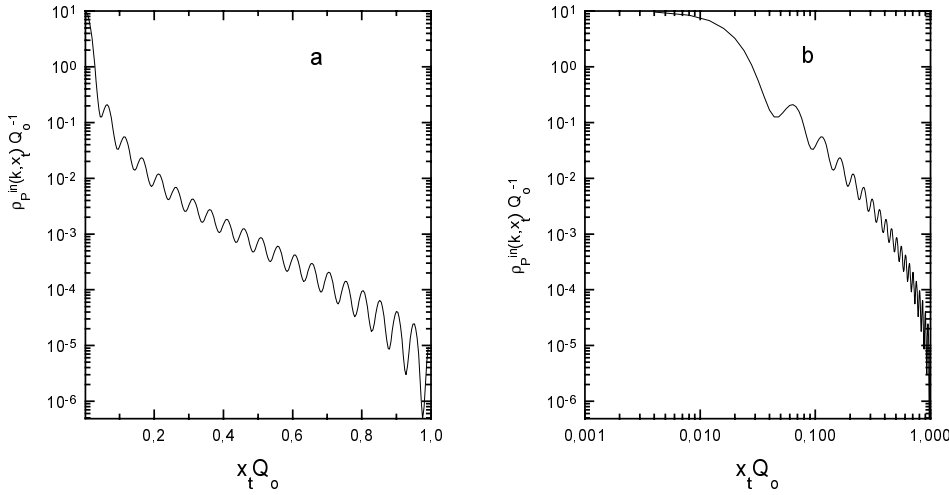
Fig. 7. Function $\rho_P^{in,(1)}(k, \mathbf{x}_t, 0)$ from (52) vs. $x_T \equiv | \mathbf{x}_T |$ for parameters as in Fig. 6. The power fit reads $\rho_P^{in}(k, \mathbf{x}_T, 0) = (Q_0 x_T)^{-3.07} * (4.0E - 05) Q_0$. Plot **a** with the logarithmic scale for the vertical axis, plot **b** with the logarithmic scale for both vertical and horizontal axes

$$= \frac{2b}{2\pi k^3} \int \frac{ds_n}{s_n} \int \frac{d\Omega_n}{2\pi \theta_{n-1,n}^2}$$

$$\times \Theta_{n-1}(s_n) \frac{1}{\theta_{nk'}\theta_{nk}} \Theta_n(k')\Theta_n(k); \qquad (52)$$

where the index (i) refers to the vector $\mathbf{s}_i$. Taking into account phase space restriction and dominating contribution of $\frac{1}{\theta_{nk'}\theta_{nk}}$ (see Appendix C) expression (52) can be approximated as:

$$\frac{2b}{2\pi k^3} \int \frac{ds_n}{s_n} \int \frac{d\Omega_n}{2\pi \theta_{n-1,n}^2} \Theta_{n-1}(s_n) \frac{1}{\theta_{nk'}\theta_{nk}} \Theta_n(k')\Theta_n(k)$$

$$= \frac{2b}{2\pi k^3} \ln(\frac{s_{n-1}}{k}) \frac{1}{\theta_{n-1,k'}\theta_{n-1,k}} \Theta_{n-1}(k')\Theta_{n-1}(k)$$

$$\times \int_0^\infty dx_n x_n J_0(x_n \theta_{kk'}) \int_{\frac{Q_0}{k}}^{\theta_{n-1,k}} d\theta_{nk} J_0(x_n \theta_{nk})$$

$$\times \int_{\frac{Q_0}{k}}^{\theta_{n-1,k'}} d\theta_{nk'} J_0(x_n \theta_{nk'}). \qquad (53)$$

Scheme (53) can be repeated iteratively in (39). After some transformations one obtains finally (for details see Appendix C, D):

$$\rho_P^{in}(k, \mathbf{x}_{\mathbf{T(P)}}, 0)$$

$$= \frac{2b}{2\pi} k \, \Theta(\frac{Q_0}{\theta} < k < P) \int_{\frac{Q_0}{k}}^{\theta} d\theta_{Pk}$$

$$\times \int_{\frac{Q_0}{k}}^{\theta} d\theta_{Pk'} \frac{1}{2\pi} \int_0^{2\pi} d\varphi_{k'k} \, J_0(k\theta_{k'k}x_T)$$

$$I_0\left(\sqrt{8b \ln(\frac{P}{k})\left\{\int_0^\infty dx x J_0(x\theta_{kk'}) \int_{\frac{Q_0}{k}}^{\theta_{Pk}} da J_0(xa) \int_{\frac{Q_0}{k}}^{\theta_{Pk'}} da' J_0(xa')\right\}}\right)$$

$$= \frac{2b}{2\pi} k \, \Theta(\frac{Q_0}{\theta} < k < P) \int_{\frac{Q_0}{k}}^{\theta} d\theta_{Pk}$$

$$\times \int_{\frac{Q_0}{k}}^{\theta} d\theta_{Pk'} \frac{1}{2\pi} \int_0^\infty \frac{d\theta_{k'k} \, \theta_{k'k}}{\Delta(\theta_{Pk}, \theta_{Pk'}, \theta_{k'k})} J_0(k\theta_{k'k}x_T)$$

$$\times I_0\left(\sqrt{8b \ln(\frac{P}{k})\left\{\int_{\frac{Q_0}{k}}^{\theta_{Pk}} da \int_{\frac{Q_0}{k}}^{\theta_{Pk'}} da' \frac{1}{2\pi\Delta(a,a',\theta_{k'k})}\right\}}\right); \qquad (54)$$

where $\theta_{k'k}$ denotes the angle between momenta $\mathbf{k'}$, $\mathbf{k}$, which in the reference frame with the z-axis placed along P direction takes the simple form:

$$\theta_{k'k} = \sqrt{\theta_{Pk'}^2 + \theta_{Pk}^2 - 2\,\theta_{Pk'}\theta_{Pk}\cos(\varphi_{k'k})}; \qquad (55)$$

$\varphi_{k'k}$ denotes the azimuthal angle between $\mathbf{k_T}$ and $\mathbf{k'_T}$, and $\Delta(a, b, c)$ denotes the area of the triangle with sides a, b, c. The numerical plot of (54) is presented in Fig. 8. There is a limiting maximum value for $x_T = 0$, as expected, and for large x_T the function has a power decrease with the best fit exponent $x_T^{-2.43}$. The result confirms our intuitive analysis from Sect. 4.1. Density $\rho_P^{in}(k, \mathbf{x}_{\mathbf{T(P)}}, 0)$ is concentrated around the **P** direction, stronger than $\rho_P^{in}(k, \mathbf{k_T})$ from (49). The function oscillates around its power-law profile. As already mentioned in Sect. 4.1., this effect is due to the sharp cut-offs of form (9) which restrict the integration space.

Comparing (54) with the single particle density in momentum space (49), we get the same dependence on the energy k, as expected. The complicated emission term (see Fig. 9):

$$2b \ln\left(\frac{P}{k}\right) \left\{\int_0^\infty dx x J_0(x\theta_{kk'})\right.$$

$$\times \int_{\frac{Q_0}{k}}^{\theta_{Pk}} da J_0(xa) \int_{\frac{Q_0}{k}}^{\theta_{Pk'}} da' J_0(xa')\right\}$$

$$= \int d^3s \frac{k^3}{s^3} A_{ss}(k, \mathbf{k'}_T; k, \mathbf{k}_T) \qquad (56)$$

corresponds to the logarithm $\ln \frac{k_T}{Q_0}$ of (49). In fact, after integration of $\rho_P^{in}(k, \mathbf{x}_{\mathbf{T(P)}}, 0)$ over d^2x_T one obtains the same result as for (49) integrated over d^2k_T. The density $\rho_P^{in}(k, \mathbf{x}_{\mathbf{T(P)}}, 0)$ is positively defined, as well. Using the Bessel function identities from Appendix D, (54) can be
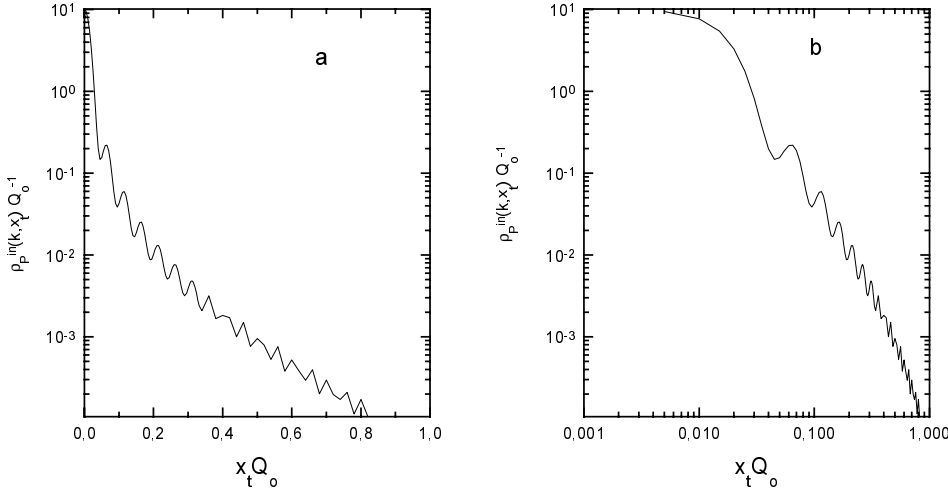
Fig. 8. Function $\rho_P^{in}(k, \mathbf{x}_t, 0)$ from (54) vs. $x_T \equiv | \mathbf{x}_T |$ for parameters as in Fig. 6. Plot **a** with the logarithmic scale for the vertical axis, plot **b** with the logarithmic scale for both vertical and horizontal axes. The power fit reads $\rho_P^{in}(k, \mathbf{x}_T, 0) = (Q_0 x_T)^{-2.43} * 0.00018 \, Q_0$

rewritten in the form:

$$
\rho_P^{in}(k, \mathbf{x_{T(P)}}, 0)
$$
$$
= \frac{2b}{2\pi} k \Theta(\frac{Q_0}{\theta} < k < P) \sum_{n=0}^{\infty} \frac{(2b)^n}{(n!)^2} \ln^n \left(\frac{P}{k}\right)
$$
$$
\times \left(\int_0^\infty dx_1 x_1 \ldots \int_0^\infty dx_n x_n\right) \sum_{m_1 \ldots m_n = -\infty}^{\infty}
$$
$$
\times \left\{ \int_{\frac{Q_0}{k}}^{\theta} d\theta_{Pk} J_{m_1}(x_1 \theta_{Pk}) \ldots J_{m_n}(x_n \theta_{Pk}) \right.
$$
$$
\left. \times J_{m_1 + \ldots + m_n}(x_T k \theta_{Pk}) \prod_{i=1}^{n} \int_{\frac{Q_0}{k}}^{\theta_{Pk}} da_i J_0(x_i a_i) \right\}^2 ; \quad (57)
$$

which implies positive definitness. For $x_T = 0$ $\rho_P^{in}(k, \mathbf{x_{T(P)}}, 0)$ reaches its maximal value, as expected. Diagramatically, formula (54) represents the chain of independent emission factors (56) transformed onto the transverse x_T plane by the Bessel factor of primary emission from the parent P, namely $J_0(| \mathbf{k}_T - \mathbf{k}'_T | x_T)$ (see Fig. 10). For $k = P$ expression (54) reduces to (51) with the dominance of the primary emission, as expected.

5 Summary

We considered the QCD parton cascade created in $e^+ e^-$ collision in the double logarithmic approximation. Using the density matrix (DM) formalism [9], and restricting ourselves to the terms leading in the double logarithmic (DL) perturbative expansion for the quasi-diagonal limit $k' \cong k$, we derived the explicit form of the inclusive single particle density matrix $d_P^{in}(k', k)$ and single particle density $\rho_P^{in}(k, \mathbf{x_{T(P)}}, 0)$ (see Fig. 8) in mixed coordinates $(k_L \approx k, \mathbf{x}_T)$. The gluon density $\rho_P^{in}(k, \mathbf{x_{T(P)}}, 0)$ fulfills important physical requirements such as positive definitness and proper normalization. It is concentrated around the **P** direction, and shows the power law profile for large $\mathbf{x}_T$.
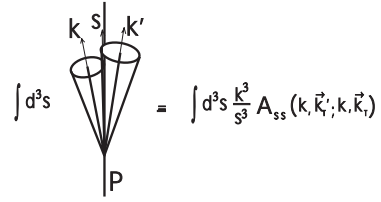

Fig. 9. Diagramatic representation of the term
$2b \ln \left(\frac{P}{k}\right) \left\{ \int_0^\infty dx x J_0(x \theta_{kk'}) \int_{\frac{Q_0}{k}}^{\theta_{Pk}} da J_0(xa) \right.$
$\left. \times \int_{\frac{Q_0}{k}}^{\theta_{Pk'}} da' J_0(xa') \right\} = \int d^3 s \frac{k^3}{s^3} A_{ss}(k, \mathbf{k}'_T; k, \mathbf{k}_T);$
The integration region lies in the overlap of conus $\Theta_s(k)$ and conus $\Theta_s(k')$

Fig. 10. Diagramatic representation of $\rho_P^{in}(k, \mathbf{x}_t, 0)$ from (54) as the chain of independent emission factors (56) transformed onto the transverse x_T plane by the Bessel factor of primary emission from the parent P, namely $J_0(| \mathbf{k}_T - \mathbf{k}'_T | x_T)$

Due to the cut-offs of the type (9) which restrict kinematic regions, the density oscillates around its power law profile. The above properties are consistent with qualitative expectations.

The above results give a positive outlook for the future. The simplified technique for calculating multiparticle observables in DLA for the constant α_S is ready. It may allow one to investigate the structure of the QCD cascade in a very comprehensive way: the exact form of a

Wigner function already would give us clear experimental predictions.

In order to improve the approach one needs to include the momentum dependence of α_S. The exact analysis of applicability of the quasi-diagonal approximation $k' \cong k$ would be required, as well. There is also a problem as to what extent the kinematical constraints characteristic for a given QCD approach (in DLA they are of the form (9)) influence the results obtained in the approach. In other words, there is a problem how to separate the effects of the kinematical restriction from the dynamical content of QCD space. The explanation would require performing an analysis similar to the presented above for LLA and MLLA schemes, as well. The MLLA approximation would be of special interest since it would incorporate the energy conservation into the cascade.

Appendix A

In DLA there are four different tree graphs M_a, M_b, M_c, M_d, describing the production of two gluons. They are defined on non-overlapping kinematic regions (see Fig. 3). Emitted gluons are either angular (AO) or energy ordered (EO).

Let us consider all the diagrams contributing to the single particle density matrix $d_P^{ex}(k'_1, k_1)$. From the (AO) and (EO) it follows that the interference between any two different graphs will appear only if either energies ω_1, ω'_1 or emission angles $\theta_{1P}, \theta_{1'P}$ of produced gluons are *strongly* ordered (Fig. 4).

This statement can be generalized for any m-particle density matrix by induction. If we have m particles, and (m-1) ones among them are "close" to each other, i.e. $k_1 \cong k'_1, \ldots, k_{m-1} \cong k'_{m-1}$, then the interference of the different diagrams will take place only if either energies or angles of k_m and k'_m are strongly ordered.

Appendix B

We shall find such terms in expansion (36) which dominate in the double logarithmic perturbative limit of $d_P^{in}(k', k)$, i.e. when $b \to 0$ ($b \propto \alpha_S$) and $P \to \infty$, so that $b \ln \frac{P}{Q_0} \to 0$ and $b \ln^2 \frac{P}{Q_0} \approx 1$, and generate double logarithmic corrections to the cross section. First let us introduce the following notation:

$$d_P^{in}(k', k) = \sum_{n=0}^{\infty} a_n; \qquad (58)$$

where coefficients a_n describe the nth order iteration of $g_S(k', k)$ (36) in the form:

$$a_n = (2b)^n \int \frac{ds_1}{s_1} \int \frac{d\Omega_{s_1}}{2\pi\theta_{Ps1}^2} \Theta_P(s_1)$$
$$\ldots \int \frac{ds_n}{s_n} \int \frac{d\Omega_{s_n}}{2\pi\theta_{n-1,n}^2} \Theta_{s_{n-1}}(s_n) g_{s_n}(k', k). \quad (59)$$

The term a_0 of the series (59) is equal to $g_P(k', k)$. Expanding it in the powers of coupling constant b, one obtains the term of the first (lowest) order of b in the form:

$$a_0^{(1)} \equiv g_P^{(1)}(k', k)$$
$$= \frac{2b}{2\pi} \frac{1}{\sqrt{k^3 k'^3}} \frac{1}{\theta_{Pk'}\theta_{Pk}} \Theta_P(k') \Theta_P(k). \qquad (60)$$

Denoting the other terms by the symbol $a_0^{(>1)} \equiv g_P^{(>1)}(k', k)$, the term a_0 from the series (59) can be rewritten as:

$$a_0 = a_0^{(1)} + a_0^{(>1)}. \qquad (61)$$

We have checked that $a_0^{(1)}$ dominates in (61). To see this, one should rewrite a_0 as:

$$a_0 \equiv g_P(k', k) = a_0^{(1)} + a_0^{(>1)} \qquad (62)$$
$$= a_0^{(1)} f(k', k; P); \qquad (63)$$

where the exact form of $f(k', k; P)$ follows from (37). For $b > 0$ and P finite the $f(k', k; P)$ vs $| \mathbf{k} - \mathbf{k}' |$ is a gauss-like function with the maximum equal to 1 for $\mathbf{k} = \mathbf{k}'$ and a non-zero minimal value. In the DL perturbative limit: $f(k', k; P) \overset{\text{PT}}{\to} 1$. Consequently, for any k, k', P:

$$a_0 \leq a_0^{(1)}, \qquad (64)$$

$$\frac{a_0}{a_0^{(1)}} \overset{\text{PT}}{\to} 1. \qquad (65)$$

Since $a_0^{(1)}$ dominates in a_0, we expect that the iterations of $a_0^{(1)}$ will generate the leading contributions to the $d_P^{in}(k', k)$. Let us introduce the notation:

$$d_P^{in,\,(1)}(k', k) = \sum_{n=0}^{\infty} a_n^{(1)}, \qquad (66)$$

$$d_P^{in,\,(>1)}(k', k) = \sum_{n=0}^{\infty} a_n^{(>1)}; \qquad (67)$$

where $a_n^{(>1)}$ and $a_n^{(1)}$ represent the result of nth iteration (59) of $a_0^{(>1)}$ and $a_0^{(1)}$ respectively. From (64) immediately follows the relation:

$$a_n = a_n^{(1)} + a_n^{(>1)} \leq a_n^{(1)}. \qquad (68)$$

Since $a_n \geq 0$, for the density matrix one obtains:

$$0 \leq d_P^{in}(k', k)$$
$$= d_P^{in,\,(1)}(k', k)$$
$$+ d_P^{in,\,(>1)}(k', k) \leq d_P^{in,\,(1)}(k', k). \qquad (69)$$

In the limit $| \mathbf{k} - \mathbf{k}' | \to 0$ the density matrix $d_P^{in}(k', k) \to d_P^{in,\,(1)}(k', k)$, and therefore:

$$\frac{d_P^{in}(k', k)}{d_P^{in,(1)}(k', k)} \overset{\text{PT}}{\to} 1. \qquad (70)$$

For other (larger) values of $\mid \mathbf{k} - \mathbf{k}' \mid$ the contribution of $d_P^{in,(1)}(k',k)$ generally need not to dominate. However, taking into account the fact that the density matrix approach works only for the quasi-diagonal limit, we may identify the quasi-diagonal region with the region of the dominance of $d_P^{in,(1)}(k',k)$. Furthermore, since $d_P^{in,(>1)}(k,k) = 0$, the $d_P^{in,(1)}(k',k)$ generates all DL corrections to the cross section. Hence we finally arrive at the relation (39).

Appendix C

To transform (52) into (53) we will apply the pole approximation method ([11] and references therein). The phase space restrictions $\Theta_{n-1}(n)\Theta_n(k)\Theta_n(k')$ in (52), in particular the angular ordering (AO) $\theta_{n-1,n} \gg \theta_{n,k}$, $\theta_{n-1,n} \gg \theta_{n,k'}$ make the the term $\frac{1}{\theta_{nk'}\theta_{nk}}$ be dominating in (52). Applying the Bessel function identity [13]:

$$\int \frac{d\Omega_n}{2\pi} = \frac{1}{2\pi}\int \frac{d\theta_{nk}\,d\theta_{nk'}\,\theta_{nk}\,\theta_{nk'}}{\Delta(\theta_{nk},\theta_{nk'},\theta_{kk'})}$$
$$= \int_0^\infty dx\,x J_0(x\theta_{k'k})\int d\theta_{nk}\theta_{nk}\,J_0(x\theta_{nk})$$
$$\times \int d\theta_{nk'}\theta_{nk'}\,J_0(x\theta_{nk'}); \quad (71)$$

where $\theta_{k'k}$ denotes the relative angle between vectors $\mathbf{k},\mathbf{k}'$, and $\Delta(\theta_{nk},\theta_{nk'},\theta_{kk'})$ equals the area of triangle with sides $\theta_{k'k}$, $\theta_{k'n}$, θ_{kn}, we may rewrite expression (52) in the form:

$$\frac{2b}{2\pi k^3}\int \frac{ds_n}{s_n}\int \frac{d\Omega_n}{2\pi\theta_{n-1,n}^2}\Theta_{n-1}(n)\frac{1}{\theta_{nk'}\theta_{nk}}\Theta_n(k')\Theta_n(k)$$
$$= \frac{2b}{2\pi k^3}\int \frac{ds_n}{s_n}\int_0^\infty dx_n x_n J_0(x_n\theta_{kk'})$$
$$\times \int d\theta_{nk}J_0(x_n\theta_{nk})\int d\theta_{nk'}J_0(x_n\theta_{nk'})$$
$$\times \frac{1}{\theta_{n-1,n}^2}\Theta_{n-1}(n)\Theta_n(k')\Theta_n(k). \quad (72)$$

Because of angular ordering the angle $\theta_{n-1,n}$ practically does not change while integrating over angles $\theta_{nk}, \theta_{nk'}$, and can be successfully approximated by the angle $\theta_{n-1,k}$ ($\theta_{n-1,k'}$). Applying all the integration restrictions explicitly, we arrive finally at the expression:

$$\frac{2b}{2\pi k^3}\int \frac{ds_n}{s_n}\int \frac{d\Omega_n}{2\pi\theta_{n-1,n}^2}\Theta_{n-1}(n)\frac{1}{\theta_{nk'}\theta_{nk}}\Theta_n(k')\Theta_n(k)$$
$$= \frac{2b}{2\pi k^3}\frac{1}{\theta_{n-1,k'}\theta_{n-1,k}}\Theta_{n-1}(k')\Theta_{n-1}(k)\int_k^{s_{n-1}}\frac{ds_n}{s_n}$$
$$\times \int_0^\infty dx_n x_n J_0(x_n\theta_{kk'})\int_{\frac{Q_0}{k}}^{\theta_{n-1,k}}d\theta_{nk}J_0(x_n\theta_{nk})$$
$$\times \int_{\frac{Q_0}{k}}^{\theta_{n-1,k'}}d\theta_{nk'}J_0(x_n\theta_{nk'}); \quad (73)$$

which after trivial integration over s_n gives identity (53).

Appendix D

For our purposes let us quote the following identities for Bessel functions ([14] and references therein):

$$J_0(x\theta_{k'k}) = \sum_{m=-\infty}^\infty e^{im(\varphi-\varphi')}J_m(x\theta_{kP})J_m(x\theta_{k'P}), \quad (74)$$

$$e^{ikx\cos\varphi} = \sum_{m=-\infty}^\infty i^m e^{im\varphi}J_m(kx), \quad (75)$$

$$\int_0^\infty dx\,xJ_0(xa)J_0(xa') = \frac{\delta(a-a')}{a}; \quad (76)$$

where $\theta_{k'k}$ denotes the relative angle between momenta $\mathbf{k}'$ $\mathbf{k}$, which in the reference frame with the z-axis placed along P direction takes form (55), and $\varphi_{k'k} = \varphi-\varphi'$, where the angles φ, φ' denote the azimuthal angles of vectors $\mathbf{k_T}$ and $\mathbf{k'_T}$ on the transversal plane respectively.

Now let us repeat the scheme (52)$\to$ (53) iteratively in (39). Then, after introducing the explicit form of Fourier transform we arrive at the expression:

$$\rho_P^{in}(k,\mathbf{x_{T(P)}},0) \quad (77)$$
$$= \frac{1}{(2\pi)^2}\int d(k\theta_{kP})\,k\theta_{kP}\int d(k\theta_{kP})\,k\theta_{kP}$$
$$\times \int_0^{2\pi}d\varphi\int_0^{2\pi}d\varphi' e^{-ik\theta_{kP}x_T\cos\varphi+ik\theta_{k'P}x_T\cos\varphi'}$$
$$\times \sum_{n=0}^\infty \frac{(2b)^n}{n!}\ln^n\left(\frac{P}{k}\right)\frac{2b}{2\pi k^3}\frac{1}{\theta_{Pk}\theta_{Pk'}}\Theta_P(k)\Theta_P(k')$$
$$\times \left(\int_0^\infty dx_1 x_1 J_0(x_1\theta_{k'k})\ldots\int_0^\infty dx_n x_n J_0(x_n\theta_{k'k})\right)$$
$$\times \left\{\int_{\frac{Q_0}{k}}^{\theta_{Pk}}da_1 J_0(x_1 a_1)\int_{\frac{Q_0}{k}}^{\theta_{Pk'}}da_1' J_0(x_1 a_{1'})\right.$$
$$\left.\ldots\int_{\frac{Q_0}{k}}^{\theta_{n-1,k}}da_n J_0(x_n a_n)\int_{\frac{Q_0}{k}}^{\theta_{n-1,k'}}da_n' J_0(x_n a_n')\right\}.$$

It looks still quite complicated, however one can notice that the term in brackets:

$$\left\{\int_{\frac{Q_0}{k}}^{\theta_{Pk}}da_1 J_0(x_1 a_1)\int_{\frac{Q_0}{k}}^{\theta_{Pk'}}da_1' J_0(x_1 a_{1'})\right.$$
$$\left.\ldots\int_{\frac{Q_0}{k}}^{\theta_{n-1,k}}da_n J_0(x_n a_n)\int_{\frac{Q_0}{k}}^{\theta_{n-1,k'}}da_n' J_0(x_n a_n')\right\}; \quad (78)$$

which contains integration of 2n Bessel functions, simplifies significantly if one adds to (77) some extra off-diagonal terms, which are equal to 0 in the quasi-diagonal limit. Namely:

$$\{\ \} \stackrel{\text{DLA}}{=} \frac{1}{n!}\int_{\frac{Q_0}{k}}^{\theta_{Pk}}da_1 J_0(x_1 a_1)\int_{\frac{Q_0}{k}}^{\theta_{Pk'}}da_1' J_0(x_1 a_{1'})$$
$$\ldots\int_{\frac{Q_0}{k}}^{\theta_{Pk}}da_n J_0(x_n a_n)\int_{\frac{Q_0}{k}}^{\theta_{Pk'}}da_n' J_0(x_n a_n'). \quad (79)$$

Then expression (77) takes the simpler form:

$$
\rho_P^{in}(k, \mathbf{x_{T(P)}}, 0)
$$
$$
= \frac{2b}{2\pi}\, k\, \Theta(\frac{Q_0}{\theta} < k < P)\frac{1}{(2\pi)^2}
$$
$$
\times \int_{\frac{Q_0}{k}}^{\theta} d\theta_{kP} \int_{\frac{Q_0}{k}}^{\theta} d\theta_{k'P} \int_0^{2\pi} d\varphi
$$
$$
\times \int_0^{2\pi} d\varphi' e^{-ik\theta_{kP}x_T \cos\varphi + ik\theta_{k'P}x_T \cos\varphi'}
$$
$$
\times \sum_{n=0}^{\infty} \frac{(2b)^n}{(n!)^2} \ln^n\left(\frac{P}{k}\right) \left\{\int_0^{\infty} dx x J_0(x\theta_{k'k})\right.
$$
$$
\left.\times \int_{\frac{Q_0}{k}}^{\theta_{Pk}} da J_0(xa) \int_{\frac{Q_0}{k}}^{\theta_{Pk'}} da' J_0(xa')\right\}^n . \quad (80)
$$

Let us perform the integration over the angles φ, φ'. Replacing all the terms of the type $J_0(x\theta_{k'k})$ by their expansions (74), expanding then Fourier transforms in terms of (75), and performing the integration over φ, φ' explicitly, we arrive at (57).

However, the part of expression (57) containing Bessel functions can be rewritten as:

$$
\left(\prod_{i=1}^{n} \sum_{m_i=-\infty}^{\infty} J_{m_i}(x_i\theta_{Pk}) J_{m_i}(x_i\theta_{Pk'})\right)
$$
$$
\times J_{m_1+...+m_n}(x_T k\theta_{Pk}) J_{m_1+...+m_n}(x_T k\theta_{Pk'})
$$
$$
= \frac{1}{2\pi}\int_0^{2\pi} d\varphi_{k'k}\left(\prod_{i=1}^{n} J_0(x_i\theta_{k'k})\right) J_0(x_T k\theta_{k'k}); \quad (81)
$$

where $\varphi_{k'k}$ denotes the relative angle between the vectors $\mathbf{k}_T, \mathbf{k}'_T$ and $\theta_{k'k} = \sqrt{\theta_{Pk'}^2 + \theta_{Pk}^2 - 2\theta_{Pk'}\theta_{Pk}\cos(\varphi_{k'k})}$, as usual. Substituting (81) into (57) finally we obtain (54).

References

1. R. Hanbury-Brown, R.Q. Twiss, Nature (London) **177**, 27 (1956)
2. D.H. Boal, C.-K. Gelbke, B.K. Jennings, Rev. Mod. Phys. **62**, 553 (1990)
3. W. Ochs, J. Wosiek, Phys. Letters B**305**, 144 (1993); Y.U. Dokshitzer, I. Dremin, Nucl. Phys. B**402**, 139 (1993); P. Brax, J.-L. Meunier, R. Peschanski, Z. Phys. **C62**, 649 (1994); R. Peschanski, Multiparticle Dynamics 1992, World Scientific 1993
4. Yu.L. Dokshitzer, V.A. Khoze, A.H. Mueller, S.I. Troyan, Basics of Perturbative QCD, Editions Frontiers, Gif-sur-Yvette Cedex, France 1991 and references therein
5. Ya.I. Azimov, Yu.L. Dokshitzer, V.A. Khoze, S.I. Troyan, Z. Phys. C**27**, 65 (1985); C**31**, 231 (1986)
6. Yu.L. Dokshitzer, Phys. Letters B**305** (1993), 295 and references therein
7. J.-L. Meunier, R. Peschanski, INLN-96-01 and references therein
8. A. Bialas, M. Krzywicki, Phys. Letters B**354** (1995) 134
9. B. Ziaja, Acta Phys. Polonica B**27** (1996), 2179
10. V.S. Fadin, Yad. Fiz. **37**, 408 (1983); Yu.L. Dokshitzer, V.S. Fadin, V.A. Khoze, Z. Phys. C**15**, 325 (1982), C**18**, 37 (1983)
11. J. Wosiek, Acta Phys. Polonica B **24** (1993), 1027; W. Ochs, J. Wosiek, Phys. Letters B305, 144 (1993)
12. P.M. Morse, H. Feshbach, Methods of Theoretical Physics I, edited by McGraw-Hill Book Company, Inc. 1953, 453
13. A.H. Mueller, Nucl. Phys. B**415** (1994), 373–385
14. J.D. Jackson, *Classical Electrodynamics*, edited by J. Wiley & Sons 1975